Direction-dependent parity-time phase transition and nonreciprocal amplification with dynamic gain-loss modulation

Alex Y. Song,[1] Yu Shi,[1] Qian Lin,[2] and Shanhui Fan[1,*]
[1]*Department of Electrical Engineering, Stanford University, Stanford, California 94305, USA*
[2]*Department of Applied Physics, Stanford University, Stanford, California 94305, USA*

(Received 31 March 2018; revised manuscript received 13 July 2018; published 14 January 2019)

We show that a dynamic gain-loss modulation in an optical structure can lead to a direction-dependent parity-time ($\mathcal{PT}$) phase transition. The phase transition can be made thresholdless in the forward direction, and yet remains with a nonzero threshold in the backward direction. As a result, nonreciprocal directional amplification can be realized. Such a dynamic gain-loss modulation can be directly integrated with a semiconductor laser to provide optical isolation for the laser.

DOI: 10.1103/PhysRevA.99.013824

I. INTRODUCTION

There have been significant recent interests in the fundamental quantum physics related to parity-time ($\mathcal{PT}$) symmetry, as well as in the applications of $\mathcal{PT}$ symmetry in both optical and electromagnetic structures [1–12]. In particular, the connection between $\mathcal{PT}$ symmetry and nonreciprocity has been extensively discussed [13–21]. Optical structures exhibiting $\mathcal{PT}$ symmetry are typically described by scalar, time-independent dielectric functions. These structures cannot exhibit any nonreciprocity in their linear optical properties [13,14,22,23]. In order to achieve nonreciprocal response, most existing works exploit the significant nonlinearity enhancement provided by the $\mathcal{PT}$ phase transition [13,15–20]. Nevertheless, it has been shown that nonlinear nonreciprocal devices are fundamentally constrained by dynamic reciprocity, which significantly limits the practical functionalities of these devices [24].

In this paper, we propose an alternative route to achieve nonreciprocity in $\mathcal{PT}$-symmetric structures. We show that nonreciprocal directional amplification can arise in structures under a dynamic material gain-loss modulation. In particular, the gain-loss modulation induces a direction-dependent $\mathcal{PT}$ phase transition that is thresholdless in the forward direction [8,12,25], but with a nonzero threshold in the backward direction. Consequently, nonreciprocal directional amplification and complete optical isolation can be achieved in the linear regime in the $\mathcal{PT}$ system.

Related to our work, it has been shown that the dynamic modulation of the real part of the dielectric constant can be used to construct optical isolators and circulators [26–29]. The underlying dynamics in the systems in Refs. [26–29], however, is Hermitian and is qualitatively different from the non-Hermitian physics that we discuss here, which arise from the modulation of the imaginary part of the dielectric constant. Nonreciprocal directional amplification has been theoretically considered in Refs. [30–35], and experimentally implemented using Josephson junctions or optomechanical interactions [33,34,36,37]. None of these works, however, made use of $\mathcal{PT}$-symmetry concepts. Our approach points to a previously unrecognized connection between $\mathcal{PT}$ symmetry and nonreciprocal physics. From a practical point of view, unlike all existing approaches to directional amplification, the proposed scheme here does not rely upon the use of resonators and is inherently broadband. Furthermore, the gain-loss modulation is more straightforwardly integrable with standard semiconductor laser structures, and can be employed to protect laser sources from back-propagating noises.

II. THEORY

A. Dynamic material gain-loss modulation

To illustrate the basic concept, we consider the dielectric waveguide structure schematically shown in Fig. 1(a). The gain and loss in the waveguide is modulated as a function of space and time. Mathematically, we can represent the modulation in gain and loss by a time-varying conductivity as

$$\tilde{\sigma}(x,z,t) = \delta\sigma\, f(x)\cos(qz - \Omega t + \phi). \tag{1}$$

Here, $\delta\sigma$ is the modulation strength. $f(x)$ is the modulation profile in the x direction. q is the wave vector. Ω is the modulation frequency. ϕ is the modulation phase. We assume $f(x)$ is an odd function of x. In a laser waveguide, gain and loss modulations can be achieved by controlling the pumping levels at different positions.

The waveguide without modulation has a photonic band structure as shown in Fig. 1(b), which has two bands of modes that are even or odd with respect to the center plane of the waveguide. The field profiles of these modes are shown in the inset of Fig. 1(b). Here, for simplicity we consider only transverse-electric modes, which have the electric field perpendicular to the xz plane. In general, the modulation profile in Eq. (1) can couple modes from the two bands with opposite symmetry, with their frequencies separated by Ω. Considering only two modes involved in the coupling, the

*shanhui@stanford.edu

 ©2019 American Physical Society

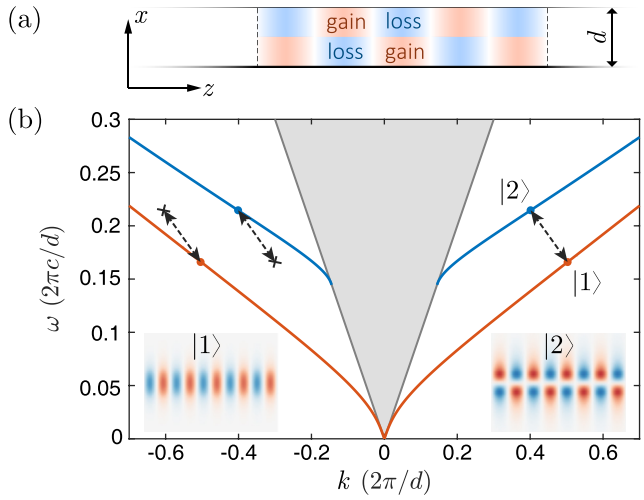

FIG. 1. (a) Schematic of a dielectric waveguide under gain-loss modulation. The waveguide has a width of d. Gain-loss modulation is applied in the region indicated between the dashed lines. (b) Band structure of the dielectric waveguide. The red (light gray) and blue (dark gray) curves show the even and the odd bands. The light cone is indicated by the shaded region. Modes $|1\rangle$ and $|2\rangle$ in the forward ($k > 0$) propagating direction are coupled by the gain-loss modulation. Insets: the electric field modal profile of modes $|1\rangle$ and $|2\rangle$, respectively.

electric field in the waveguide can be written as

$$E(x,z,t) = a_1|1\rangle + a_2|2\rangle,$$
$$|1,2\rangle = E_{1,2}(x)e^{i(k_{1,2}z-\omega_{1,2}t)}, \tag{2}$$

where $E_{1,2}(x)$ is the modal profile in x, which are normalized so that $|a_{1,2}|^2$ are the intensity of the respective modes. k and ω are the wave vector and the frequency of each mode. Defining $\psi(z) = (a_1(z), a_2(z))^T$, the equation of motion in the modulated waveguide can be derived using coupled mode theory [26]:

$$i\partial_z\psi(z) = H(z)\psi(z),$$
$$H(z) = \begin{pmatrix} 0 & -iCe^{i\Delta kz - i\phi} \\ -iCe^{-i\Delta kz + i\phi} & 0 \end{pmatrix}, \tag{3}$$

where $\Delta k = k_2 - k_1 - q$ is the wave-vector mismatch, and $C = \frac{\delta\sigma}{8}\int f(x)E_1(x)E_2(x)dx$ is the coupling strength.

B. Direction-dependent $\mathcal{PT}$ phase transition

Equation (3) is in the form of a time-periodic Schrödinger equation with z taking the role of time. The Hamiltonian $H(z)$ satisfies the $\mathcal{PT}$ symmetry defined as [38–41]

$$\mathcal{P} = \begin{pmatrix} 1 & 0 \\ 0 & -1 \end{pmatrix}; \quad \mathcal{T}H(z)\mathcal{T}^{-1} = H^*(-z). \tag{4}$$

The definition of $\mathcal{P}$ stems from the fact that mode $|1\rangle$ is even under parity operation, while mode $|2\rangle$ is odd.

As a result of the $\mathcal{PT}$ symmetry, the Floquet quasienergies of the system must be either real or complex-conjugate pairs. A proof can be found in Appendix A. To obtain the Floquet eigenstates and the quasienergies, we first solve for the evolution operator $U(z,0)$ defined by $\psi(z) = U(z,0)\psi(0)$:

$$U(z,0) = \begin{pmatrix} e^{i\Delta kz/2}\left(\cosh C'z - i\frac{\Delta k/2}{C'}\sinh C'z\right) & -e^{-i\phi}e^{i\Delta kz/2}\frac{C}{C'}\sinh C'z \\ -e^{i\phi}e^{-i\Delta kz/2}\frac{C}{C'}\sinh C'z & e^{-i\Delta kz/2}\left(\cosh C'z + i\frac{\Delta k/2}{C'}\sinh C'z\right) \end{pmatrix}, \tag{5}$$

where $C' = \sqrt{C^2 - (\Delta k/2)^2}$. Then, the quasienergy ϵ of the system can be obtained by letting $e^{-i\epsilon\zeta}\psi(0) = U(\zeta,0)\psi(0)$, where $\zeta = 2\pi/\Delta k$ is the period of the Hamiltonian along z. The obtained quasienergies are

$$\epsilon_\pm = \frac{\Delta k}{2} \pm C\sqrt{\left(\frac{\Delta k}{2C}\right)^2 - 1} \quad (\text{mod } \Delta k). \tag{6}$$

From Eq. (6), we observe that the system has a $\mathcal{PT}$ phase transition controlled by the ratio $\Delta k/2C$ as shown in Fig. 2(a). If the wave-vector mismatch dominates over the coupling strength, i.e., $\Delta k > 2C$, the system is in the exact $\mathcal{PT}$ phase. Both quasienergies are real, and the Floquet eigenmodes do not experience gain or loss. On the other hand, for small wave-vector mismatch, i.e., $\Delta k < 2C$, the system is in the broken phase where the quasienergies of the system split into complex-conjugate pairs. Thus, one of the Floquet modes will be amplified in the system.

We now consider a gain-loss modulation that provides a phase-matched coupling between two modes with different wave vectors in the forward direction as illustrated in Fig. 1(b). Such a modulation introduces a direction-dependent $\mathcal{PT}$ phase transition as is shown in Fig. 2(b). In the forward direction, $\Delta k_f = k_1 - k_2 - q = 0$. From Eq. (6), the quasienergies become $\epsilon_\pm = \pm iC$. Thus, the quasienergies split into complex-conjugate pairs as soon as coupling strength C increases from 0, i.e., the system exhibits a thresholdless $\mathcal{PT}$ phase transition [10,12,25]. For the backward direction, however, $\Delta k_b \neq 0$, and the gain-loss modulation does not provide phase-matched coupling between any pair of modes. Thus, the system exhibits a $\mathcal{PT}$ phase transition with a nonzero threshold in the backward direction.

C. Nonreciprocal directional gain

Such a direction-dependent $\mathcal{PT}$ phase transition gives rise to the effect of nonreciprocal directional amplification in this system. To illustrate this effect, we consider the regime where $\Delta k_f = 0$, and $\Delta k_b \gg C$. Under these conditions, the evolution operator can be simplified as

$$U_f = \begin{pmatrix} \cosh Cz & -e^{-i\phi}\sinh Cz \\ -e^{i\phi}\sinh Cz & \cosh Cz \end{pmatrix},$$
$$U_b = \begin{pmatrix} 1 & 0 \\ 0 & 1 \end{pmatrix}, \tag{7}$$

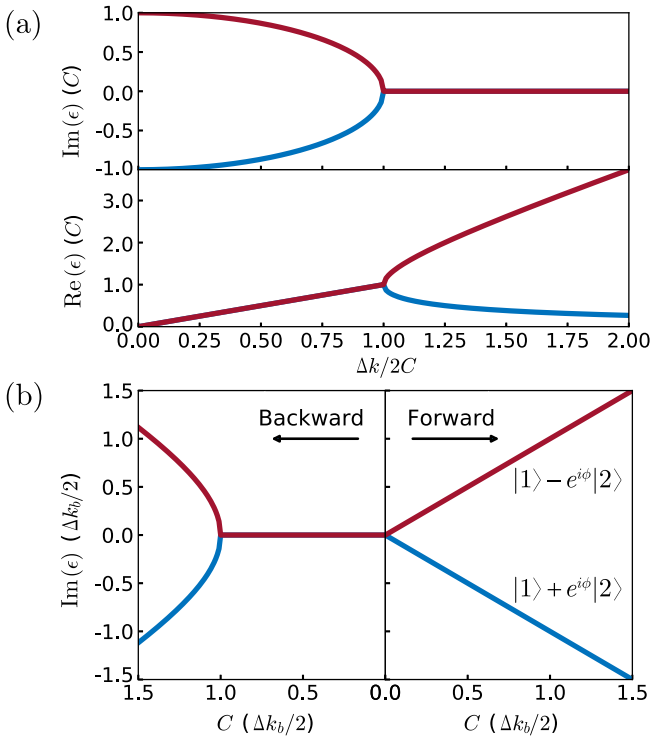

FIG. 2. (a) Real and imaginary parts of the Floquet quasienergies as a function of $\Delta k/2C$. For large phase mismatch ($\Delta k/2C > 1$), the system is in the exact $\mathcal{PT}$ phase where the quasienergies are real. For small phase mismatch ($\Delta k/2C < 1$), the system is in the broken phase. (b) Direction-dependent $\mathcal{PT}$ phase transition for the structure shown in Fig. 1. For the backward direction, due to strong phase mismatch, the system is in the exact $\mathcal{PT}$ phase for modulation strength $C \leqslant \Delta k_b/2$. For forward direction where $\Delta k = 0$, the system is in $\mathcal{PT}$ broken phase for any nonzero modulation strength.

where f, b stand for forward and backward propagations, respectively. In the forward direction, one of the Floquet eigenmodes $|1\rangle - e^{i\phi}|2\rangle$ is amplified, while the other mode $|1\rangle + e^{i\phi}|2\rangle$ is attenuated. Thus, if $|1\rangle$ is the input to the waveguide, then the output becomes $\cosh(Cz)|1\rangle - e^{i\phi}\sinh(Cz)|2\rangle$, providing amplification to the input mode. In fact, input in the forward direction with any modal profile including $|1\rangle$, $|2\rangle$ or any of their combinations, except $|1\rangle + e^{i\phi}|2\rangle$, will be amplified. In contrast, the system is in the exact $\mathcal{PT}$ phase in the backward direction. The Floquet eigenmodes are $|1\rangle$ and $|2\rangle$, with both quasienergies approaching 0. Thus, an input mode in the backward direction, with any modal profile, does not experience any gain or loss.

We notice that in general the system described by Eq. (3) is non-Hermitian, and the evolution operator U is not unitary. Thus, in general, mode propagation in the system does not preserve mode orthogonality or the total energy flux. Instead, for any Δk, the evolution operator U in Eq. (5) is symplectic satisfying $\det(U) = 1$. Hence, with any input mode profile, the intensity difference between modes $|1\rangle$ and $|2\rangle$ is always conserved. Such a symplectic dynamics is qualitatively different from the previously studied unitary dynamics in systems undergoing modulations in the real part of the dielectric function [26].

III. NUMERICAL DEMONSTRATION

In the following, we numerically demonstrate the nonreciprocal effects predicted above using finite-difference time-domain (FDTD) simulations. We assume a waveguide with a permittivity of $\varepsilon = 12.75$, and a width of $d = 1$. We select two modes of the waveguide as shown in Fig. 1(b). Mode $|1\rangle$ has a frequency of $\omega_1 = 0.165$ and a wave vector of $k_1 = 0.5$, while mode $|2\rangle$ has $\omega_2 = 0.213$ and $k_2 = 0.4$. The frequencies and the wave vectors are normalized to $2\pi c_0/d$ and $2\pi/d$, respectively. All the lengths below are normalized to d. A section of the waveguide with a length of $l = 20$ is under gain-loss modulation. The modulation has a frequency $\Omega = 0.048$ and a wave vector $q = 0.1$, chosen to match the two modes in the forward direction. The modulation strength $\delta\sigma$ is 1. We input a Gaussian pulse in mode $|1\rangle$ from either left or right with a normalized peak intensity of 1 as shown in Fig. 3(a). In the forward direction, the input mode $|1\rangle$ evolves into a linear superposition of $|1\rangle$ and $|2\rangle$, as is shown in Fig. 3(a). The intensity in both modes $|1\rangle$ and $|2\rangle$ exceeds unity, indicating the presence of amplification. The intensity difference between the modes $|1\rangle$ and $|2\rangle$ remains unity, in agreement with the conservation law derived analytically above. In the backward direction, however, the input mode $|1\rangle$ passes through without amplification or attenuation as is shown in Fig. 3(b), again in agreement with the analytical results derived above. The numerical simulation here thus provides a validation of the theory presented above.

In the structure shown in Fig. 3, the direction-dependent amplification for the even mode is accompanied by the generation of amplitudes in the odd mode. To provide a single-mode response with directional amplification, one can use a passive reciprocal structure to filter out the odd mode. An example is shown in Fig. 4, where we have used a tapered waveguide region as a modal filter [42–45]. The tapered region has the same dielectric constant as the waveguide. It has a length of 25, and its width linearly changes from 1 to 0.5. As is shown in Fig. 4(a), in the forward direction, an input mode $|1\rangle$ is amplified by the gain-loss modulation region. Then, since the generated mode $|2\rangle$ is not guided in the narrower part of the tapered region, it leaks out of the waveguide, leaving an amplified mode $|1\rangle$ at the output on the right side. In contrast, in the backward direction, input mode $|1\rangle$ propagates through the tapered region and the modulated region without any amplification, as is shown in Fig. 4(b). We note such a filter scheme is based on the modal profile rather than the frequency and hence can preserve the broadband nature of the device, even in the case where the modulation frequency is small.

IV. DEVICE APPLICATION

A. Optical isolation

With directional gain available, it is straightforward to construct nonreciprocal optical isolation. One can connect the gain-loss modulation region with a lossy waveguide region, so that the wave has a net unit transmission in one direction, while it is attenuated in the other direction. Both such lossy waveguides, as well as the tapered waveguide region as

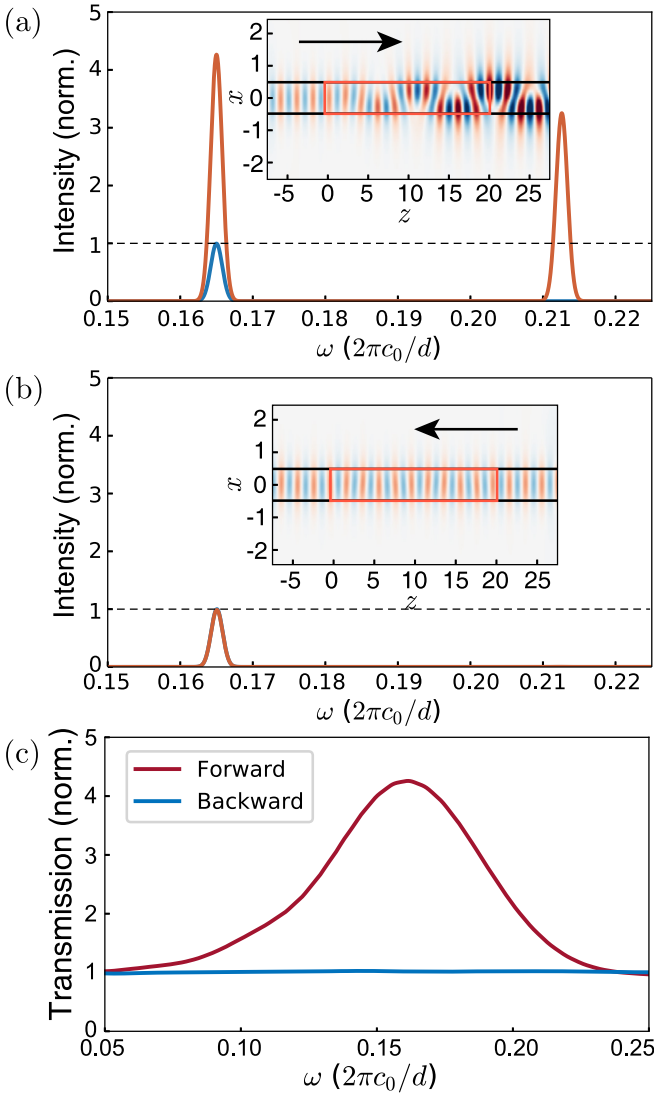

FIG. 3. (a), (b) Transmission of an input pulse in mode $|1\rangle$ in the forward and backward directions, respectively. The intensity spectrum of the input pulse is shown by the blue (dark gray) curve. The output spectra are shown by the red (light gray) curves. Electric field distribution is shown in the insets of (a) and (b), in which the wave propagation direction is marked by the black arrow. The gain-loss modulated region is indicated in the red (gray) rectangle. (c) The mode-to-mode transmission coefficient spectrum from mode $|1\rangle$ to mode $|1\rangle$ in the forward (red or light gray) and backward (blue or dark gray) directions, respectively.

discussed above, are reciprocal elements and are standard in integrated photonic circuits.

We emphasize here that any semiconductor laser system, by its very construction, already has the mechanism to introduce gain-loss modulations since the gain or loss of the active medium depends on the applied pumping. Thus, an isolator based on our approach can be directly integrated into the laser structure. This could significantly simplify the integration of semiconductor lasers into integrated photonic circuits.

It is also important to note that the performance of the scheme here, i.e., the contrast ratio of the nonreciprocal transmission, scales with the device length. Thus, the strength

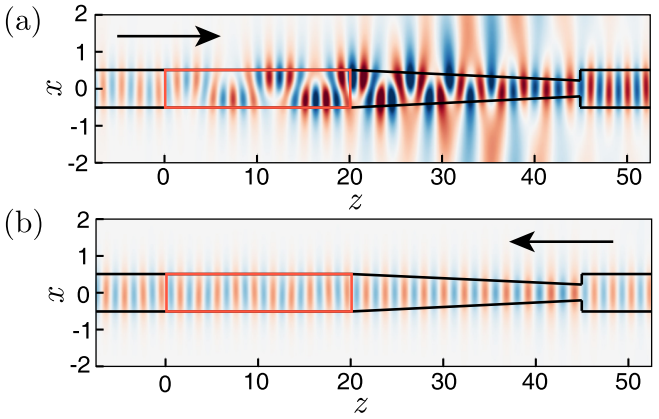

FIG. 4. A visualization of the directional gain in a waveguide with gain-loss modulation (marked by the red rectangle) and a tapered region. The electric field distribution for the forward and backward propagation waves are shown in (a) and (b), respectively. The width of the linearly tapered region changes from 1 to 0.5. The field is only amplified in the forward direction in (a) but not reversed in (b).

of the optical isolation here can be arbitrarily set according to demand, by adjusting the device length.

B. Broadband operation

The nonreciprocal directional amplification discussed here can operate over a broad bandwidth, provided that modes $|1\rangle$ and $|2\rangle$ are in the parallel region of the even and odd bands in Fig. 1(b). Then, if a gain-loss modulation induces a phase-matched coupling between two modes with ω_1, k_1 and ω_2, k_2, it also induces a phase-matched coupling between modes $\omega_1 + \delta\omega, k_1 + \delta k$ and $\omega_2 + \delta\omega, k_2 + \delta k$ [26]. As a demonstration, in Fig. 3(c) we show the the mode-to-mode transmission spectrum for the even mode $|1\rangle$ in both directions. In the forward direction, the transmission exceeds unity in a broad frequency range of 0.06–0.24, while in the backward direction the transmission is nearly constant at 1. Thus, significant nonreciprocal directional gain can occur in a broad frequency range with its width comparable to its center frequency. As a result, in practical device applications, the operation bandwidth will only be limited by the gain bandwidth of the materials. The broadband characteristics here is in contrast with existing schemes on directional amplifications, which are all based on resonant interactions and hence are inherently narrow banded.

C. Realistic device design

In the above demonstration, we have assumed a modulation frequency of $\Omega/\omega \approx 0.3$, and a modulation strength of $\delta\sigma = 1$, which corresponds to a modulation strength in the imaginary part of permittivity of $\delta\varepsilon_i/\varepsilon = \delta\sigma/\omega\varepsilon \approx 0.1$. In today's semiconductor laser technology, the achievable modulation frequency is a few tenths of gigahertz [46], corresponding to a smaller modulation frequency of $\Omega/\omega \approx 10^{-4}$. The gain coefficient in these lasers typically reaches well over 5×10^3 cm^{-1} [47], corresponding to a large gain-loss modulation strength of $\delta\varepsilon_i/\varepsilon \gtrsim 0.1$. Thus, the assumed modulation

strength in the numerical demonstration is within the current experimental capabilities.

We note that in today's semiconductor laser technology in the telecommunication wavelength range [46], the achievable modulation frequency can reach above 50 GHz. For a laser operating at 1.55 μm, if we assume the applied gain-loss modulation is phase matched for the forward direction, then the wave-vector mismatch in the backward direction is $\Delta k_b = 72\ \mathrm{cm}^{-1}$ [26]. To ensure the backward direction is in the $\mathcal{PT}$ unbroken phase, i.e., with no gain or loss, the coupling strength must satisfy $2C \leqslant \Delta k_b$. Thus, the maximal allowed C is 36 cm^{-1}. Recall that $\pm iC$ are the Floquet quasienergies in the forward direction, i.e., C is the gain coefficient of the modes in the forward direction. 36 cm^{-1} translates into around 15 dB/mm.

The required modulation strength $\delta\sigma$ can be calculated using $C = \frac{\delta\sigma}{8}\int f(x)E_1(x)E_2(x)dx$, where $f(x) = 1$ for $0 < x \leqslant d/2$ and $f(x) = -1$ for $-d/2 < x \leqslant 0$. $E_{1,2}(x)$ are the modal profiles. The effective modulation strength in the imaginary part of the permittivity can then be approximated by $\delta\varepsilon_i \approx \delta\sigma/\omega$, where ω is the frequency of light at 1.55 μm. This gives a modulation strength of $\delta\varepsilon_i/\varepsilon \approx 1.0 \times 10^{-3}$. Such a modulation strength is readily achievable with today's semiconductor laser technology.

In a realistic semiconductor laser waveguide, changes in the real part of the refractive index can sometimes accompany the gain-loss modulations. There are a number of experimental situations where the strength of gain-loss modulation is significantly larger than the strength of associated index modulation [48–52]. For these situations, our discussion here focusing only on the gain-loss modulation is a good approximation. In the case where both index and gain-loss modulations exist, the nonreciprocal gain-loss effect still persists in the system. Additional information can be found in Appendix B.

V. CONCLUSION

In summary, we have shown that dynamic gain-loss modulations in a dielectric waveguide structure can give rise to a direction-dependent $\mathcal{PT}$ phase transition that is thresholdless in the forward direction but with a nonzero threshold in the backward direction. As a result, nonreciprocal directional gain and complete optical isolation can be achieved in the linear regime. This mechanism of direction-dependent $\mathcal{PT}$ phase transition is a previously unexplored connection between $\mathcal{PT}$ symmetry and nonreciprocal physics. The obtained nonreciprocal gain effect here is broadband, and the isolator structure is directly integrable with standard semiconductor lasers. The performance of such a device scales with its length, thus can be controlled based on needs. Further exploration of this connection may offer new opportunities in studying novel non-Hermitian topological physics in dynamic and nonreciprocal systems [53–57].

ACKNOWLEDGMENT

This work is supported by US Air Force Office of Scientific Research (Grants No. FA9550-16-1-0010 and No. FA9550-17-1-0002).

APPENDIX A: QUASIENERGY OF FLOQUET $\mathcal{PT}$-SYMMETRIC SYSTEM

We assume $H(x,t)$ is the Hamiltonian of a non-Hermitian Floquet system satisfying $H(t+\tau) = H(t)$. We further assume $H(x,t)$ satisfies the following $\mathcal{PT}$ symmetry:

$$\begin{aligned}\mathcal{P}: &\quad \hat{x} \to -\hat{x}, \quad \hat{p} \to \hat{p},\\ \mathcal{T}: &\quad \hat{x} \to \hat{x}, \quad \hat{p} \to -\hat{p}, \quad i \to -i, \quad t \to -t.\end{aligned} \tag{A1}$$

Using the Floquet theorem, we write the Floquet eigenstate in the following form:

$$\psi(x,t) = e^{-i\epsilon t}\phi(x,t), \tag{A2}$$

where $\phi(x,t) = \phi(x,t+\tau)$, ϵ is the Floquet quasienergy, and

$$[H(x,t) - i\partial_t]\phi(x,t) = \epsilon\phi(x,t). \tag{A3}$$

Since H satisfies the $\mathcal{PT}$ symmetry, we have

$$\mathcal{PT}[H(x,t) - i\partial_t](\mathcal{PT})^{-1}\mathcal{PT}\phi(x,t) = \mathcal{PT}\epsilon\phi(x,t),$$

which leads to

$$[H(x,t) - i\partial_t]\phi^*(-x,-t) = \epsilon^*\phi^*(-x,-t), \tag{A4}$$

which means ϵ^* is also a Floquet quasienergy, with the eigenmode $e^{-i\epsilon^* t}\phi(-x,-t)$.

APPENDIX B: A SYSTEM UNDER BOTH INDEX AND GAIN-LOSS MODULATIONS

Here, we perform a numerical simulation of the scenario that both index and gain-loss modulations exist in a waveguide. The setup is similar to that shown in Fig. 3 of the main text, except that we now add a modulation in the real part of the permittivity, denoted $\tilde{\varepsilon}(x,z,t)$, with the same modulation strength as the imaginary part,

$$\tilde{\varepsilon}(x,z,t) = \delta\varepsilon f(x)\sin(qz - \Omega t + \phi). \tag{B1}$$

Here, $\delta\varepsilon = 1$, $f(x)$ is the modulation profile in the x direction, q is the wave vector. Ω is the modulation frequency, ϕ is the modulation phase. The transmission spectra of the structure in both directions are plotted in Fig. 5. It is observed that, in the presence of both index and gain-loss modulations, the system still shows a contrast in the transmission coefficient of mode $|1\rangle$ in the forward and backward directions. Thus, the nonreciprocal gain-loss effect still persists in this scenario.

In a waveguide where the gain-loss modulation and the refractive index modulation are introduced in separate sections, the system can exhibit other interesting effects. For example, such a system can generate a nonreciprocal transmission in a single mode, without producing any associated secondary modes. To demonstrate this, we apply a gain-loss modulation (red or light gray) followed by a index modulated section (blue or dark gray) in the setup shown in Fig. 6. The modulation strength, frequency, and wave vector for the gain-loss modulated section are the same as those in Fig. 3. The index modulated section employs the same modulation frequency and wave vector, with a modulation depth of $\delta\varepsilon = 1$. In the forward direction, the gain-loss modulation can amplify an input mode $|1\rangle$, at the same time generate mode $|2\rangle$. Then, the following index modulation section can rotate the photons

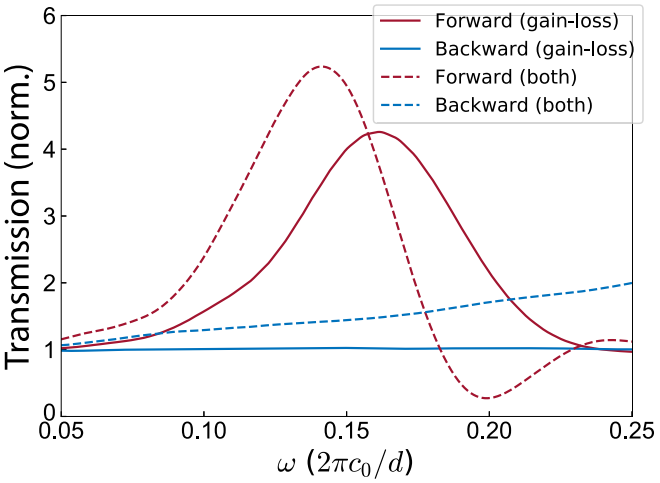

FIG. 5. Comparison of purely gain-loss modulations to both index and gain-loss modulations. The solid curves are the transmission spectra of mode $|1\rangle$ with gain-loss modulations only, while the dashed curves are that of both index and gain-loss modulations.

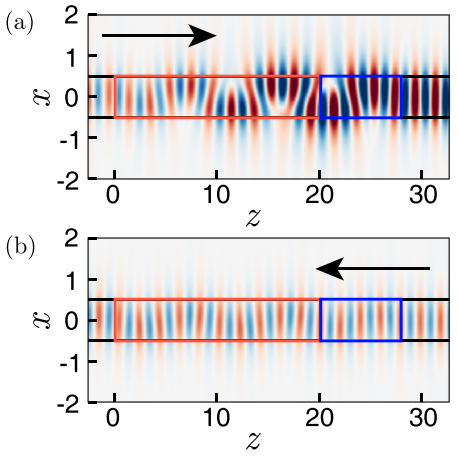

FIG. 6. A waveguide with a gain-loss modulated section (red or light gray) followed by an index modulated section (blue or dark gray). The gain-loss modulated section has a length of 20, and the index modulated section has a length of 8. The direction of wave propagation is marked in the black arrow.

in mode $|2\rangle$ to mode $|1\rangle$. The net effect is an amplified mode $|1\rangle$ only. In the backward direction, however, mode $|1\rangle$ propagates through the two sections without invoking mode $|2\rangle$ due to wave-vector mismatch. The system thus exhibits nonreciprocal amplification in mode $|1\rangle$ only, without any other associated modes.

[1] C. M. Bender and S. Boettcher, Phys. Rev. Lett. **80**, 5243 (1998).
[2] K. G. Makris, R. El-Ganainy, D. N. Christodoulides, and Z. H. Musslimani, Phys. Rev. Lett. **100**, 103904 (2008).
[3] A. Guo, G. J. Salamo, D. Duchesne, R. Morandotti, M. Volatier-Ravat, V. Aimez, G. A. Siviloglou, and D. N. Christodoulides, Phys. Rev. Lett. **103**, 093902 (2009).
[4] C. E. Rüter, K. G. Makris, R. El-Ganainy, D. N. Christodoulides, M. Segev, and D. Kip, Nat. Phys. **6**, 192 (2010).
[5] Z. Lin, H. Ramezani, T. Eichelkraut, T. Kottos, H. Cao, and D. N. Christodoulides, Phys. Rev. Lett. **106**, 213901 (2011).
[6] Y. D. Chong, L. Ge, and A. D. Stone, Phys. Rev. Lett. **106**, 093902 (2011).
[7] S. Bittner, B. Dietz, U. Günther, H. L. Harney, M. Miski-Oglu, A. Richter, and F. Schäfer, Phys. Rev. Lett. **108**, 024101 (2012).
[8] L. Feng, Y.-L. Xu, W. S. Fegadolli, M.-H. Lu, J. E. B. Oliveira, V. R. Almeida, Y.-F. Chen, and A. Scherer, Nat. Mater. **12**, 108 (2013).
[9] Y. Lumer, Y. Plotnik, M. C. Rechtsman, and M. Segev, Phys. Rev. Lett. **111**, 263901 (2013).
[10] L. Feng, Z. J. Wong, R.-M. Ma, Y. Wang, and X. Zhang, Science **346**, 972 (2014).
[11] H. Hodaei, M.-A. Miri, M. Heinrich, D. N. Christodoulides, and M. Khajavikhan, Science **346**, 975 (2014).
[12] A. Cerjan, A. Raman, and S. Fan, Phys. Rev. Lett. **116**, 203902 (2016).
[13] Y. Huang, Y. Shen, C. Min, S. Fan, and G. Veronis, Nanophotonics **6**, 977 (2017).
[14] X. Yin and X. Zhang, Nat. Mater. **12**, 175 (2013).
[15] X. Zhou and Y. D. Chong, Opt. Express **24**, 6916 (2016).
[16] H. Ramezani, T. Kottos, R. El-Ganainy, and D. N. Christodoulides, Phys. Rev. A **82**, 043803 (2010).
[17] B. Peng, S. K. Özdemir, F. Lei, F. Monifi, M. Gianfreda, G. L. Long, S. Fan, F. Nori, C. M. Bender, and L. Yang, Nat. Phys. **10**, 394 (2014).
[18] L. Chang, X. Jiang, S. Hua, C. Yang, J. Wen, L. Jiang, G. Li, G. Wang, and M. Xiao, Nat. Photonics **8**, 524 (2014).
[19] F. Nazari, N. Bender, H. Ramezani, M. Moravvej-Farshi, D. N. Christodoulides, and T. Kottos, Opt. Express **22**, 9574 (2014).
[20] X. Zhu, H. Ramezani, C. Shi, J. Zhu, and X. Zhang, Phys. Rev. X **4**, 031042 (2014).
[21] S. Longhi, Phys. Rev. Lett. **103**, 123601 (2009).
[22] D. Jalas, A. Petrov, M. Eich, W. Freude, S. Fan, Z. Yu, R. Baets, M. Popović, A. Melloni, J. D. Joannopoulos, M. Vanwolleghem, C. R. Doerr, and H. Renner, Nat. Photonics **7**, 579 (2013).
[23] S. Fan, R. Baets, A. Petrov, Z. Yu, J. D. Joannopoulos, W. Freude, A. Melloni, M. Popovic, M. Vanwolleghem, D. Jalas, M. Eich, M. Krause, H. Renner, E. Brinkmeyer, and C. R. Doerr, Science **335**, 38 (2012).
[24] Y. Shi, Z. Yu, and S. Fan, Nat. Photonics **9**, 388 (2015).
[25] L. Ge and A. D. Stone, Phys. Rev. X **4**, 031011 (2014).
[26] Z. Yu and S. Fan, Nat. Photonics **3**, 91 (2009).
[27] D.-W. Wang, H.-T. Zhou, M.-J. Guo, J.-X. Zhang, J. Evers, and S.-Y. Zhu, Phys. Rev. Lett. **110**, 093901 (2013).
[28] M. S. Kang, A. Butsch, and P. S. J. Russell, Nat. Photonics **5**, 549 (2011).

[29] H. Lira, Z. Yu, S. Fan, and M. Lipson, Phys. Rev. Lett. **109**, 033901 (2012).
[30] A. Metelmann and A. A. Clerk, Phys. Rev. X **5**, 021025 (2015).
[31] D. Malz, L. D. Tóth, N. R. Bernier, A. K. Feofanov, T. J. Kippenberg, and A. Nunnenkamp, Phys. Rev. Lett. **120**, 023601 (2018).
[32] A. Kamal and A. Metelmann, Phys. Rev. Appl. **7**, 034031 (2017).
[33] F. Ruesink, M.-A. Miri, A. Alù, and E. Verhagen, Nat. Commun. **7**, 13662 (2016).
[34] B. Abdo, K. Sliwa, L. Frunzio, and M. Devoret, Phys. Rev. X **3**, 031001 (2013).
[35] T. T. Koutserimpas and R. Fleury, Phys. Rev. Lett. **120**, 087401 (2018).
[36] K. Fang, J. Luo, A. Metelmann, M. H. Matheny, F. Marquardt, A. A. Clerk, and O. Painter, Nat. Phys. **13**, 465 (2017).
[37] Z. Shen, Y. L. Zhang, Y. Chen, C. L. Zou, Y. F. Xiao, X. B. Zou, F. W. Sun, G. C. Guo, and C. H. Dong, Nat. Photonics **10**, 657 (2016).
[38] N. Moiseyev, Phys. Rev. A **83**, 052125 (2011).
[39] X. Luo, J. Huang, H. Zhong, X. Qin, Q. Xie, Y. S. Kivshar, and C. Lee, Phys. Rev. Lett. **110**, 243902 (2013).
[40] Y. N. Joglekar, R. Marathe, P. Durganandini, and R. K. Pathak, Phys. Rev. A **90**, 040101 (2014).
[41] M. Chitsazi, H. Li, F. M. Ellis, and T. Kottos, Phys. Rev. Lett. **119**, 093901 (2017).
[42] W. Bogaerts, D. Taillaert, B. Luyssaert, P. Dumon, J. V. Campenhout, P. Bienstman, D. V. Thourhout, R. Baets, V. Wiaux, and S. Beckx, Opt. Express **12**, 1583 (2004).
[43] K. Kasaya, O. Mitomi, M. Naganuma, Y. Kondo, and Y. Noguchi, IEEE Photonics Technol. Lett. **5**, 345 (1993).
[44] B. Corcoran, C. Monat, C. Grillet, D. J. Moss, B. J. Eggleton, T. P. White, L. O'Faolain, and T. F. Krauss, Nat. Photonics **3**, 206 (2009).
[45] J. F. Bauters, M. L. Davenport, M. J. R. Heck, J. K. Doylend, A. Chen, A. W. Fang, and J. E. Bowers, Opt. Express **21**, 544 (2013).
[46] K. Nakahara, Y. Wakayama, T. Kitatani, T. Taniguchi, T. Fukamachi, Y. Sakuma, and S. Tanaka, IEEE Photonics Technol. Lett. **27**, 534 (2015).
[47] M.-l. Ma, J. Wu, Y.-q. Ning, F. Zhou, M. Yang, X. Zhang, J. Zhang, and G.-y. Shang, Opt. Express **21**, 10335 (2013).
[48] R. R. Alexander, D. Childs, H. Agarwal, K. M. Groom, H. Y. Liu, M. Hopkinson, and R. A. Hogg, Jpn. J. Appl. Phys. **46**, 2421 (2007).
[49] P. K. Kondratko, S.-l. Chuang, G. Walter, T. Chung, and N. Holonyak, Appl. Phys. Lett. **83**, 4818 (2003).
[50] C. Gmachl, F. Capasso, D. L. Sivco, and A. Y. Cho, Rep. Prog. Phys. **64**, 1533 (2001).
[51] T. Aellen, R. Maulini, R. Terazzi, N. Hoyler, M. Giovannini, J. Faist, S. Blaser, and L. Hvozdara, Appl. Phys. Lett. **89**, 091121 (2006).
[52] C. Holly, S. Hengesbach, M. Traub, and D. Hoffmann, Opt. Express **21**, 15553 (2013).
[53] A. Cerjan, M. Xiao, L. Yuan, and S. Fan, Phys. Rev. B **97**, 075128 (2018).
[54] D. Leykam, K. Y. Bliokh, C. Huang, Y. D. Chong, and F. Nori, Phys. Rev. Lett. **118**, 040401 (2017).
[55] J. M. Zeuner, M. C. Rechtsman, Y. Plotnik, Y. Lumer, S. Nolte, M. S. Rudner, M. Segev, and A. Szameit, Phys. Rev. Lett. **115**, 040402 (2015).
[56] S. Malzard, C. Poli, and H. Schomerus, Phys. Rev. Lett. **115**, 200402 (2015).
[57] K. Esaki, M. Sato, K. Hasebe, and M. Kohmoto, Phys. Rev. B **84**, 205128 (2011).